

## Binding of deposited gold clusters to thiol self-assembled monolayers on Au(111) surfaces

Leila Costelle,<sup>1,a)</sup> Tommi T. Järvi,<sup>2</sup> Minna T. Räisänen,<sup>3,b)</sup> Vladimir Tuboltsev,<sup>1</sup> and Jyrki Räisänen<sup>1</sup>

<sup>1</sup>Department of Physics, Division of Materials Physics, University of Helsinki, P.O. Box 43, Helsinki FI-00014, Finland

<sup>2</sup>Fraunhofer-Institut für Werkstoffmechanik IWM, Wöhlerstrasse 11, D-79108 Freiburg, Germany

<sup>3</sup>EaStCHEM School of Chemistry, University of St. Andrews, North Haugh, St. Andrews KY16 9ST, United Kingdom

(Received 28 October 2010; accepted 5 January 2011; published online 27 January 2011)

We study the mechanisms involved in Au nanocluster deposition on thiol self-assembled monolayer modified Au(111) surfaces. Molecular dynamics simulations reveal a wide range of cluster-surface binding configurations within a very narrow deposition energy range (0.2–0.6 eV/atom for  $\sim 2.5$  nm diameter clusters). These go from noncovalent to full contact and include surprising intermediate cases in which the clusters are bound to the underlying Au(111) surface via molecular links and nanowires. Experiments show that, subsequently, the clusters are covered by thiols and slightly flattened. © 2011 American Institute of Physics. [doi:10.1063/1.3548862]

Nanometer-sized metal particles exhibit interesting optical, electronic, magnetic, and structural properties, the exploitation of which is of key importance in several emerging technologies.<sup>1</sup> For example, biomedical applications, sensors, and selective optical filters make use of the optical properties of gold nanoparticles, which are highly dependent on the size, shape, and degree of particle-to-particle coupling.<sup>2</sup>

Manufacturing advanced materials using clusters as building blocks requires immobilization of prefabricated nanoparticles or particle synthesis on the surface as the initial preparation step.<sup>3,4</sup> An interesting platform is provided by self-assembled monolayer (SAM) modified surfaces, which allow for tuning surface reactivity by adjusting the free terminal group of the thiol molecules.<sup>5–7</sup> In the present study, we use low-energy deposition to immobilize gas-phase gold clusters on a Au(111) substrate covered with *n*-dodecanethiol (DT) SAM. Deposition of clusters performed in the gas phase offers the possibility to control the size and morphology of the deposited clusters. By using a DT SAM, the cluster-SAM interaction can be probed without the added complication of a reactive end group on the thiol. Only a few studies have reported the deposition of gas-phase clusters on thiol-SAM/Au(111) surfaces.<sup>7–9</sup> While the penetration of the deposited clusters through the SAM can be controlled to some extent, the involved mechanisms are poorly understood.

To gain insight into the mechanisms and a better understanding of the cluster-SAM interaction, we employ molecular dynamics (MD) simulations and scanning tunneling microscopy (STM) studies.

*n*-dodecanethiol ( $\geq 98\%$ ) was purchased from Sigma-Aldrich (Finland) and used as received. Thiol SAMs were prepared at room temperature, immersing flame-annealed Au(111)-coated mica slides in 1 mM ethanol solution of

*n*-dodecanethiol for 4 h, after which the samples were rinsed with ethanol and blown dry with N<sub>2</sub>.

The gold clusters were deposited under ultrahigh vacuum using a gas aggregation source (NC200, Oxford Applied Research, United Kingdom).<sup>10</sup> Cluster coverage was controlled by the deposition time and the size distribution was determined using the grain analysis function in Gwyddion.<sup>11</sup> The samples were imaged using STM (PicoScan, Agilent Technology, USA) in constant-current mode under ambient conditions. The STM tips were mechanically cut Pt/Ir (80:20) wires, with diameters of 0.25  $\mu$ m (Advent Research Materials Ltd., UK). When imaging nano-sized particles with STM, tip-convolution effects lead to the enlargement of the apparent diameter of the particles, the effect of which was corrected as described by Schiffmann *et al.*<sup>12</sup>

The MD simulations were carried out with the LAMMPS code,<sup>13</sup> with a recently developed potential in the ReaxFF formalism,<sup>14–16</sup> the properties of which have been fit to an extensive database of *ab initio* results of gold-thiol-hydrocarbon interactions. The results were visualized using visual molecular dynamics (VMD).<sup>17</sup>

The preformed gold clusters impinge on the surface with low kinetic energy. We consider, as a rough approximation, that the cluster velocity is close to the expanding gas velocity  $V_{Ar} = [2kT\gamma/(\gamma-1)m_{Ar}]^{1/2} \approx V_{cluster}$ , with  $\gamma=5/3$  for argon,<sup>3</sup> leading to a kinetic energy of  $\sim 0.3$  eV/atom. Figure 1(a) shows a large-scale STM image of the deposited gold clusters on Au(111)/DT SAM at low coverage. The Au vacancy islands appearing as dark pits in the images are characteristic features of thiol adsorption on Au(111).<sup>18</sup> The clusters are randomly distributed, with no enhanced concentration observed at the step edges, domain boundaries, or Au vacancy islands. The possibility of cluster migration and consequent binding to the Au vacancy islands has been ruled out by a detailed analysis of the STM images and comparing the number of Au vacancy islands before and after the cluster depositions. The stability of the clusters was investigated by repeated imaging with STM (intervals of several weeks),

<sup>a)</sup>Electronic mail: leila.costelle@helsinki.fi.

<sup>b)</sup>Present address: Department of Chemistry, Laboratory of Inorganic Chemistry, University of Helsinki, P.O. Box 55, Helsinki FI-00014, Finland.

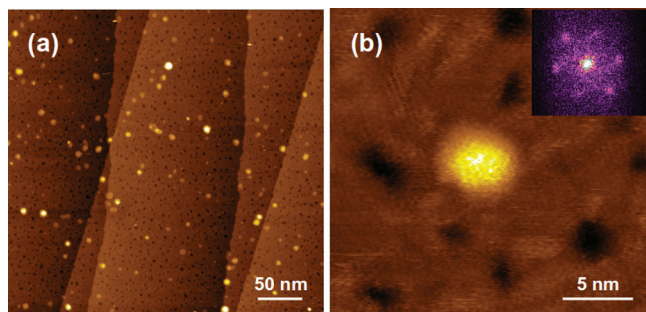


FIG. 1. (Color) (a) Large-scale STM image of deposited clusters on DT SAM/Au(111). (b) High-resolution image showing an individual Au cluster, with the corresponding FFT image in the inset.

showing unaltered morphology. The mobility of the clusters is thus negligible at room temperature. Figure 1(b) shows a high resolution image of a densely packed SAM layer on top of a deposited cluster. The thiol molecules have a typical hexagonal arrangement with a 5 Å periodicity.<sup>19</sup> Thus, the hexagonal pattern indicates that the molecules reorganize into a well-ordered SAM after deposition.

The diameters of the deposited clusters range from 1.8 to 7.5 nm and typical heights from 0.6 to 1.7 nm. No coalescence of the particles was observed at low coverage. Thus, the mean incident cluster size is  $\sim 500$  atoms (2.5 nm diameter in the spherical approximation) [Fig. 2(a)]. The effective mean cluster aspect ratio is  $\sim 5$ , indicating that the clusters undergo some flattening, but are not reduced to monolayer height, as was observed under similar conditions by Lando *et al.*,<sup>9</sup> who deposited clusters of a mean size of about 350 atoms at  $\sim 0.5$  eV/atom.

In the binding process, several mechanisms operate on different time scales. While the landing of clusters typically occurs on the time scale of picoseconds, diffusion and alkyl chain reorganization can take hours. In order to understand the mechanism underlying the penetration of the cluster through the organic layer, we have performed MD simulations to model gold cluster deposition on DT SAMs.

In the simulations, clusters of differing sizes were placed on top of a Au(111)/DT SAM layer of  $\sim (5 \times 5)$  to  $(7 \times 7)$  nm<sup>2</sup>, depending on the cluster size. Both the cluster and the substrate were equilibrated at 0 K, after the substrate is annealed at room temperature. The thiol molecules were taken to rest on the planar Au(111) surface. The cluster was then rotated randomly and given a random lateral displacement, after which it was given a velocity downward.

We start with considering simulation results for clusters of 405 atoms. As the clusters impinged on the surface, they were found to compress the alkyl chains of the underlying thiol molecules against the Au surface. For low energy

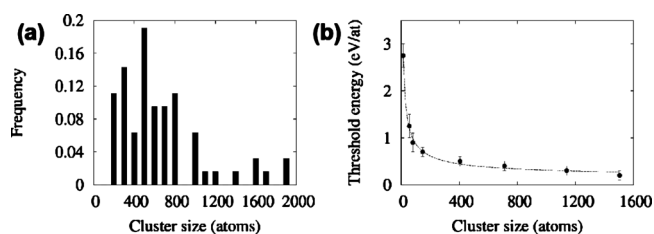


FIG. 2. (a) Experimental cluster size distribution. (b) Simulated threshold deposition energy for cluster binding on SAM as a function of cluster size. The line shows a fit of form  $E = a + bN^{-c}$ , with  $c = 0.62 \pm 0.05$ .

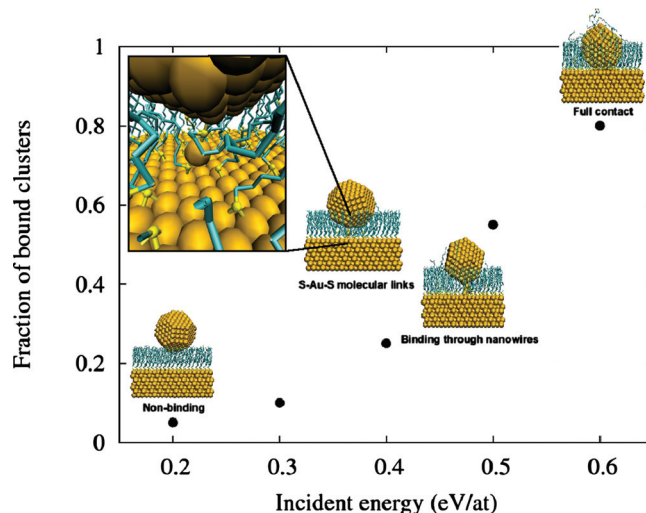


FIG. 3. (Color) Fraction of 405 atom gold clusters bound to the Au surface, either through molecular links, nanowires, or via full contact, as a function of deposition energy, with snapshots of deposition simulation showing typical binding configurations.

( $\sim 0.2$ – $0.3$  eV/atom), the compressed thiols tend to straighten, pushing the cluster away from the surface. Typically, this restoring force is so strong that it prevents covalent cluster-surface bond formation and the cluster remains embedded in the SAM. However, in some cases, as shown in the inset of Fig. 3, the cluster is bound to the Au(111) surface through a S–Au–S or similar linking unit, formed spontaneously during the deposition process. When the deposition energy is increased to 0.5 eV/atom, the force due to compressed thiols is no longer strong enough to push the clusters away from the surface and most of the clusters become bound to the surface, either through a few atom Au wires or molecular links. Finally, increasing the energy to 0.6 eV/atom leads to full contact between the cluster and the substrate (Fig. 3). Thus, a transition from nonbinding to full-binding occurs in a narrow energy interval as illustrated in Fig. 3.

Although the observation of structures bound by nanowires and molecular links is quite surprising, note that atom-thick gold wires have been demonstrated before, e.g., by breaking gold contacts.<sup>20</sup> The S–Au–S molecular links, on the other hand, are stabilized by the strong Au–S bonding.

In order to test the cluster size dependence of the deposition process, simulations were carried out for sizes from 13 to 1504 atoms. The threshold energy, above which more than half of the clusters bind to the surface covalently (either through nanowires, molecular links, or full contact) is shown in Fig. 2(b). For small clusters, high energy is needed for immobilization, the threshold quickly decreasing with increasing cluster size. The threshold energy is closely related to the projected range of a cluster as it is slowed down by the SAM. In a study concerning graphite (see Ref. 21 and references therein), the clusters range has been shown to be proportional to their momentum ( $p$ ) divided by projected area ( $R \propto p/r^2$ ). For a SAM of constant thickness  $h$ , it follows that the energy per atom required to penetrate the film scales as  $E \propto N^{-2/3}$ ,  $N$  being the number of atoms in the cluster. Indeed, fitting a curve of the form  $E = a + bN^{-c}$  to the data in Fig. 2(b) yields to  $c = 0.62 \pm 0.05$ , matching the expected scaling perfectly.

Note that no cluster flattening is observed in the simulations, contrary to our experiments and Ref. 9. This clearly shows that at the present energies, flattening does not occur directly upon deposition, but rather by diffusive processes and over longer time scales than what is accessible by MD. Further experiments have to address the question of stability of the predicted structures and the flattening mechanism by, e.g., controlling the deposition energy exactly at the low energies required and performing deposition at low temperature.

In conclusion, we presented molecular dynamics simulations and experiments of low-energy Au cluster deposition on thiol SAMs. The simulations predict, in a narrow deposition energy interval, binding structures where the clusters are bound to the underlying Au(111) surface through nanowires and molecular links. They also show similar scaling behavior of penetration of the SAM to what is observed for cluster penetration into graphite. The experiments, compared with previous studies,<sup>7-9</sup> show that not only the thiol terminal group, but also small changes in deposition energy and particle size distribution lead to large changes in, e.g., flattening kinetics of the particles upon deposition.

This work has been partly supported by the Academy of Finland (Project No. 121567). We thank Dr. Manfred Buck, University of St. Andrews for making the STM equipment available.

<sup>1</sup>*Nanoparticles: From Theory to Application*, edited by G. Schmid (Wiley, Weinheim, 2004).

<sup>2</sup>Y. Dirix, C. Bastiaansen, W. Caseri, and P. Smith, *J. Adv. Mater.* **11**, 223 (1999).

<sup>3</sup>I. Yamada, J. Matsuo, N. Toyoda, and A. Kirkpatrick, *Mater. Sci. Eng. R.*

**34**, 231 (2001).

<sup>4</sup>K. Nordlund, T. T. Järvi, K. Meinander, and J. Samela, *Appl. Phys. A: Mater. Sci. Process.* **91**, 561 (2008).

<sup>5</sup>R. Madueno, M. T. Räisänen, C. Silien, and M. Buck, *Nature (London)* **454**, 618 (2008).

<sup>6</sup>A. M. Bittner, *Surf. Sci. Rep.* **61**, 383 (2006).

<sup>7</sup>N. Vandamme, J. Snauwaert, E. Janssens, E. Vandeweert, P. Lievens, and C. V. Haesendonck, *Surf. Sci.* **558**, 57 (2004).

<sup>8</sup>R. P. Andres, T. Bein, M. Dorogi, S. Feng, J. I. Henderson, C. P. Kubiak, W. Mahoney, R. G. Osifchin, and R. Reifengerger, *Science* **272**, 1323 (1996).

<sup>9</sup>A. Lando, K. Lauwaet, and P. Lievens, *Phys. Chem. Chem. Phys.* **11**, 1521 (2009).

<sup>10</sup>In brief, a discharge was generated by a direct current magnetron equipped with a gold target and operated with a 20 SCCM (SCCM denotes cubic centimeter per minute at STP) Ar flow to generate the clusters. The magnetron power and chamber pressure were kept at 40 W and 10 Pa, respectively.

<sup>11</sup>See <http://gwyddion.net/Free> for SPM (AFM, SNOM/NSOM, STM, MFM) data analysis software.

<sup>12</sup>K. I. Schiffmann, M. Fryda, G. Goerigk, R. Lauer, and P. Hinze, *Ultramicroscopy* **66**, 183 (1996).

<sup>13</sup>S. Plimpton, *J. Comput. Phys.* **117**, 1 (1995); See <http://lammmps.sandia.gov> for LAMMPS.

<sup>14</sup>T. T. Järvi, A. C. T. van Duin, W. A. Goddard III, and K. Nordlund, (unpublished).

<sup>15</sup>T. T. Järvi, A. Kuronen, M. Hakala, K. Nordlund, A. C. T. van Duin, W. A. Goddard III, and T. Jacob, *Eur. Phys. J. B* **66**, 75 (2008).

<sup>16</sup>K. Chenoweth, A. C. T. van Duin, and W. A. Goddard III, *J. Phys. Chem. A* **112**, 1040 (2008).

<sup>17</sup>W. Humphrey, A. Dalke, and K. Schulten, *J. Mol. Graphics* **14**, 33 (1996).

<sup>18</sup>F. Schreiber, *Prog. Surf. Sci.* **65**, 151 (2000).

<sup>19</sup>F. Terán Arce, M. E. Vela, R. C. Salvarezza, and A. J. Arvia, *Electrochim. Acta* **44**, 1053 (1998).

<sup>20</sup>A. I. Yanson, R. R. Bollinger, H. E. van den Brom, N. Agrät, and J. M. van Ruitenbeek, *Nature (London)* **395**, 783 (1998).

<sup>21</sup>V. N. Popok, S. Vučković, J. Samela, T. T. Järvi, K. Nordlund, and E. E. B. Campbell, *Phys. Rev. B* **80**, 205419 (2009).